POLITECNICO DI TORINO
Repository ISTITUZIONALE

Production and characterization of single-phase diopside sol–gel powder

Original
Production and characterization of single-phase diopside sol–gel powder / Khamidov, A., Ruzimuradov, O., Batirov, D., Tulyaganov, D.U., Miola, M., Baino, F.. - In: MATERIALS LETTERS. - ISSN 0167-577X. - 355:(2024). [10.1016/j.matlet.2023.135570]

Availability:
This version is available at: 11583/2987962 since: 2024-04-22T08:07:57Z

Publisher:
Elsevier

Published
DOI:10.1016/j.matlet.2023.135570

Terms of use:

This article is made available under terms and conditions as specified in the corresponding bibliographic description in the repository

Publisher copyright
Elsevier postprint/Author's Accepted Manuscript

© 2024. This manuscript version is made available under the CC-BY-NC-ND 4.0 license http://creativecommons.org/licenses/by-nc-nd/4.0/.The final authenticated version is available online at: http://dx.doi.org/10.1016/j.matlet.2023.135570

(Article begins on next page)

26 November 2026

Production and characterization of single-phase diopside sol-gel powder

Anvar Khamidov[1], Olim Ruzimuradov[1], Davlatjon Batirov[1], Dilshat U. Tulyaganov[1], Marta Miola[2], Francesco Baino[2,*]

[1] *Department of Natural-Mathematical Sciences, Turin Polytechnic University in Tashkent, Tashkent 100095, Uzbekistan*

[2] *Institute of Materials Physics and Engineering, Department of Applied Science and Technology, Politecnico di Torino, 10129 Torino, Italy*

* Correspondence: francesco.baino@polito.it

Abstract

In this work, diopside powder was synthesized through the sol–gel method aiming at obtaining single-phase fine particles. Tetraethyl orthosilicate, calcium nitrate tetrahydrate and magnesium chloride hexahydrate were used as sources of cations, in ratios specific to diopside. Wet gel was synthesized by hydrolyzing a homogeneous solution consisting of precursors dissolved in ethanol. Ground gel powder was investigated by differential thermal analysis and thermogravimetry (DTA-TGA) to define details of the subsequent heat treatments. Samples calcined at 600, 650, 700, 800 and 1100 °C for 3 hours underwent characterization through Fourier-transform infrared spectroscopy, X-ray diffraction analysis and scanning electron microscopy. Diopside was found as the single crystalline phase in the interval 600-1100°C.

Keywords: Bioceramics; Diopside; Sol-gel; Silicates.

1. Introduction

Calcium magnesium silicates are attracting an increasing interest in the field of bioceramics due to their appealing properties for bone-contact applications, including high biocompatibility, bioactivity (i.e., apatite-forming ability) and tunable degradation rate, which can also be modulated by doping with proper metallic ions [1,2]. This class of bioceramics encompasses some well-known biomedical materials belonging the ternary system SiO_2–CaO–MgO, such as diopside ($CaMgSi_2O_6$), merwinite ($Ca_3MgSi_2O_8$) and akermanite ($Ca_2MgSi_2O_7$) [3,4]. In this regard, diopside was also found to develop as a crystalline phase in bioactive glass-ceramics with interesting bone-bonding properties due to the high ability to form hydroxyapatite (HA) in vitro [5,6] and to stimulate osteoblast proliferation in vivo [7]. It is also worth mentioning that "true" glass production from the melt of stoichiometric diopside composition is constrained by undesired phenomena associated with the high tendency towards surface nucleation during cooling, yielding the unavoidable formation of glass-ceramic products [8,9].

Diopside can be produced by different methods, including some variants of the sol-gel process [10] and co-precipitation route [11]. The easiest approach relies on wet chemistry, involving the transition from a sol to a gel followed by calcination. In this article, we report the chemical synthesis of pure diopside powders through the sol–gel method. Although several attempts were undertaken to synthesize diopside from solution [12-15], there is still the need for optimizing the sol–gel process to obtain high-purity fine particles in a controlled way.

2. Materials and methods

2.1 Synthesis

Calcium nitrate tetrahydrate ($Ca(NO_3)_2{\cdot}4H_2O$) supplied by Carlo Erba Reagents and magnesium chloride hexahydrate ($MgCl_2{\cdot}6H_2O$) by Sigma-Aldrich were selected as sources of Ca and Mg, respectively. Tetraethyl orthosilicate (TEOS, $Si(OC_2H_5)_4$) supplied by Sigma-Aldrich was used as Si precursor.

In the course of the experimental procedure, 0.025 mol each of $Ca(NO_3)_2{\cdot}4H_2O$ and $MgCl_2{\cdot}6H_2O$ were dissolved in 30 mL ethanol under magnetic stirring that continued for 1 h; then, 0.050 mol of $Si(OC_2H_5)_4$

was added. The mixture was stirred for 1.5 h until obtaining a transparent sol that was cast into Petri dish and left undisturbed for 2 h at room temperature to let the gelation and aging processes to take place. The wet gel was dried in an oven at 80 °C for 24 h and for this treatment the Petri dish was slightly opened to allow the slow evaporation of the alcoholic liquid phase. Ground gel powder was heat treated at 600, 650, 700, 800 and 1100 °C for 3 h at a heating rate of 10 °C/min and the calcined samples, after being ground, underwent characterization. Calcination temperatures were selected on the basis of previous studies [12,13] and to allow comparison with such literature; a holding time of 3 h was hypothesized to be enough to obtain only pure diopside without transient phases.

2.2 Characterizations

Differential thermal and thermogravimetric analyses (DTA-TGA) of dried gel powder were performed using a differential thermal analyzer (STA PT1600) heating the sample from 20 °C to 1100 °C at a rate of 10 °C/min.

The functional groups of calcined samples were analyzed by FTIR (FTIR Bruker Tensor 27) over the wavenumber range of 400-1600 cm^{-1}, with 256 scans and 4 cm^{-1} resolution.

Calcined samples were also analyzed by powder X-ray diffraction (XRD) using a powder X-ray diffractometer (Rigaku Miniflex 6G). The XRD measurements were performed at a scanning speed of 1°/min, a sampling width of 0.05°, and a scanning range with 2θ varying within 20.00°–40.00° using Cu Kα radiation.

Calcined powders were sputter-coated with chromium and morphologically investigated by field-emission scanning electron microscopy (FESEM, SupraTM 40 Zeiss, Germany; accelerating voltage 5 kV).

3. Results and discussion

The sol–gel process is advanced through the decomposition, hydrolysis and polycondensation of precursors and the gelation of the sol; the further stages include gel ageing, drying and calcination to finally produce ceramic powders [16]. DTA-TGA curves of the dry powder gel sample (Fig. 1) show that about 60-61 %

of its mass was lost before 500 °C while the maximum weight loss of ~64 % was attained at 800 °C. A very moderate weight loss was revealed at further heating in the interval 800-1100 °C. A very sharp endothermic peak centered at 142 °C could be ascribed to water and alcohol evaporation from the pores of the gel. Two other endothermic events at 254 and 491 °C are most likely due to the thermal decomposition of source compounds, i.e. nitrates ($Ca(NO_3)_2 \cdot 4H_2O$) and chlorides ($MgCl_2 \cdot 6\ H_2O$) used as oxide precursors in the synthesis process, in agreement with previous literature [17]. In particular, according to [18], dehydration of $Ca(NO_3)_2 \cdot 4H_2O$ to anhydrous $Ca(NO_3)_2$ starts above ~29 °C and continues up to ~202 °C. The next stage is connected with the melting of $Ca(NO_3)_2$ at 543 °C followed by its decomposition in the liquid phase to nitrogen oxide, oxygen, nitrogen and solid CaO. Thermal decomposition of $MgCl_2 \cdot 6H_2O$ was shown to comprise six steps with formation of (1) $MgCl_2 \cdot 4H_2O$ at 69 °C, (2) $MgCl_2 \cdot 2H_2O$ at 129 °C, (3) $MgCl_2 \cdot nH_2O$ ($1 \leq n \leq 2$) and MgOHCl at 167 °C, (4) $Mg(OH)Cl \cdot 0.3H_2O$ at 203 °C, (5) MgOHCl at 235 °C, and (6) direct conversion of MgOHCl to MgO at 415 °C [19].

DTA-TGA curves (Fig. 1) demonstrate that all residuals could be removed before 600 °C and, therefore, this temperature was chosen for the primary calcination of the powder samples. Onset crystallization temperature and maximum crystallization (peak) temperature were revealed at 822 and 854 °C, respectively.

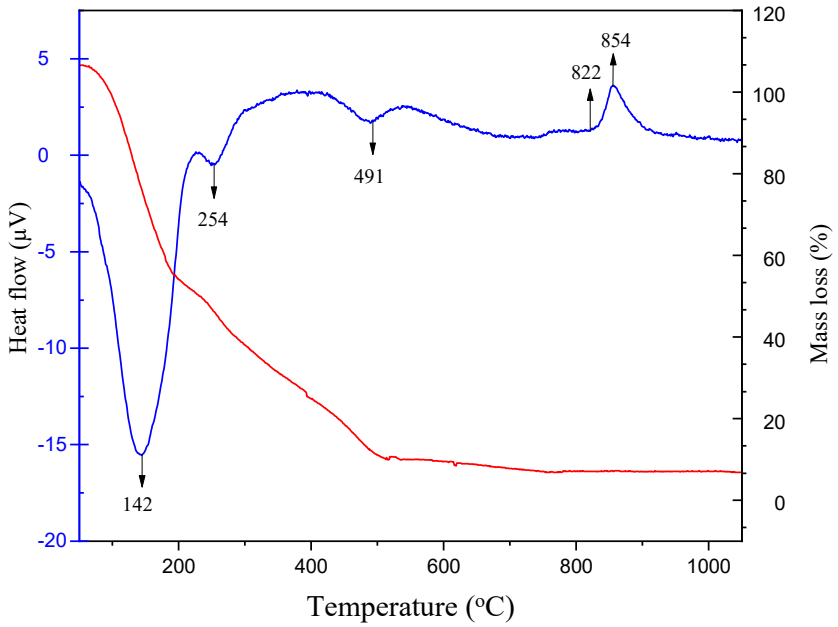

Fig. 1. DTA-TGA curves of the dry powder gel.

FTIR spectra of samples calcined at 600 °C, 800 °C and 1100 °C (Fig. 2) fairly resemble each other and are consistent with the spectrum of synthetic diopside obtained by the sol-gel combustion method [20-22]. The most intense bands associated with the diopside lie in the 800-1200 cm^{-1} region, the next between 400-600 cm^{-1}, while the least intensive lie between 600-800 cm^{-1}. In particular, the O-Si-O bending vibrations were observed at 634 and 672 cm^{-1} and the bands at 869 and 991 cm^{-1} are associated with Si-O symmetric stretching. The symmetric Si-O-Si stretching vibration was recorded at 1067 cm^{-1}. Characteristic transmittance bands for O-Ca-O and O-Mg-O non-bridging bending vibrational modes were observed at 412 cm^{-1} and at 466 to 501 cm^{-1}, respectively.

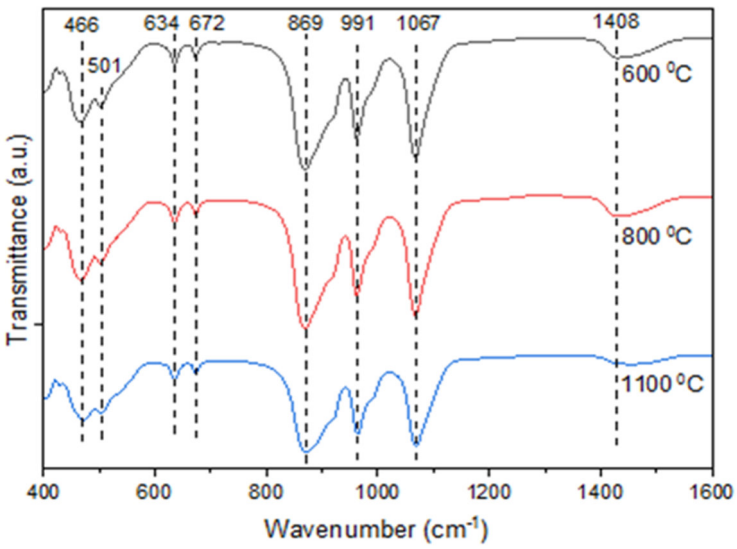

Fig. 2. FTIR spectra of samples calcined at 600 °C, 800 °C and 1100 °C

XRD results are consistent with FTIR data. The first signs of diopside precipitation were revealed at 600 °C while, on further heating, intensities of diffraction peaks significantly increased suggesting improved crystallinity. Interestingly, traces of diopside are found at lower temperatures than those predicted by DTA (<800 °C); this can be justified by the relatively long calcination time (3 h). Diopside was found as the single crystalline phase in the interval 650-1100 °C (Fig. 3), which is one of the important outcomes of the present work. On the contrary, in two previous studies on diopside synthesis by sol-gel process, Iwata et al. [12] reported that the gel powder crystallized into diopside single phase only at 1100 °C, and Yamamoto et al. [13] observed the simultaneous formation of forsterite along with diopside in the samples sintered at temperatures 650, 700 and 800 °C; in both cases, the lower calcination time compared to the present study (2 vs. 3 h) might have played a role. In another relevant study [14], TEOS and calcium/magnesium nitrates were employed as sources of cations, in ratios specific to diopside, and samples were further subjected to gelation, calcination (600 °C) and thermal treatments at 800 and 1000 °C: XRD investigation of the samples sintered at 1000 °C demonstrated that multiphase material was formed containing diopside as the major crystalline phase along with akermanite and merwinite.

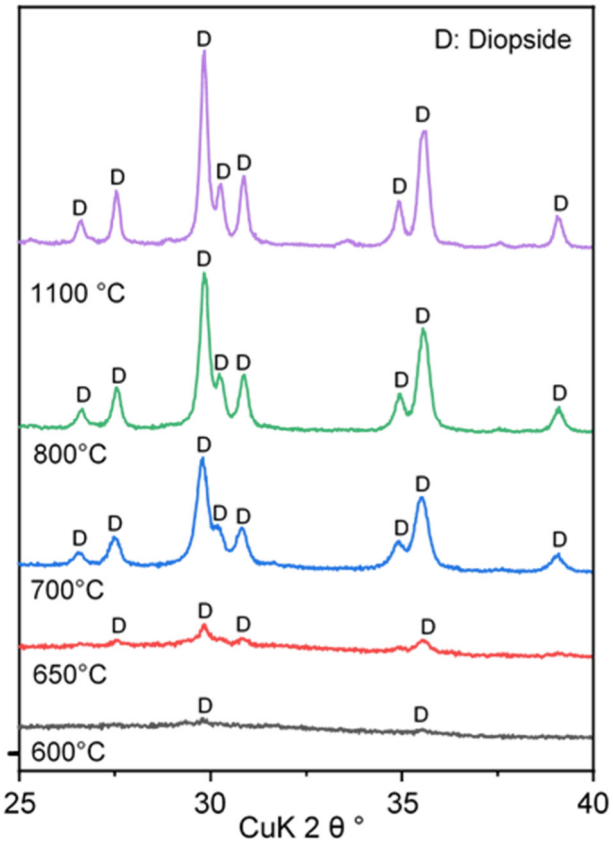

Fig. 3. XRD of samples calcined at 600, 650, 700, 800 and 1100 °C.

The morphology of samples is displayed in Fig. 4. SEM micrographs reveal the presence of submicronic nanoparticles (size in the range of 100-200 nm) with high tendency to agglomeration. The particle morphology changes as temperature increases from petal-like (600 °C) to quasi-spherical shape (1100 °C).

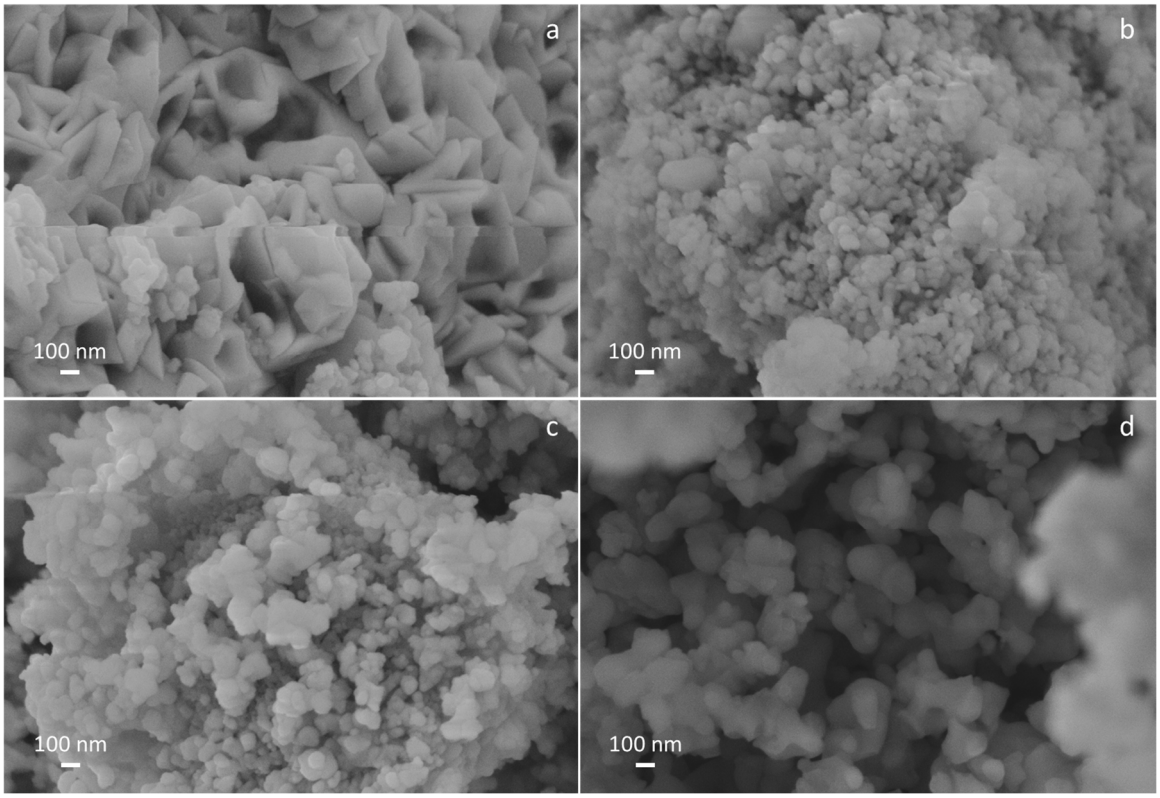

Fig. 4. Scanning electron microscopy images of the materials calcined at (a) 600, (b) 700, (c) 800 and (d) 1100 °C (magnification 100,000×).

4. Conclusions

The sol-gel synthesis route used in this study allowed producing diopside as the single crystalline phase in the calcination interval 600-1100 °C for 3 h. Specifically, submicronic particles (size 100-200 nm) were obtained, the shape of which progressively becomes more regular and spherical with the increment of the calcination temperature. Future research will be dedicated to assessing the relevant properties of these powders in the context of bone regeneration, including biomineralization ability and biological interactions with cells, as well as their potential application for fabricating high-added-value products, such as porous scaffolds.

References

[1] Z. Ba, et al., Int. J. Nanomed. 13 (2018) 3883-3896.

[2] S. Pang, et al., Mater. Des. 215 (2022) 110480.

[3] M. Ansari, et al., J. Biomim. Biomater. Biomed. Eng. 44 (2020) 73-81.

[4] Y. Hosseini, et al., Mater. Chem. Phys. 194 (2017) 356-366.

[5] S. Kapoor, et al., Acta Biomaterialia, 15, (2015) 210-226.

[6] F. Baino, et al., Ceramics 5 (2022) 120-130.

[7] A. D. Matchanov et al., Materials 15 (2022) 4197 .

[8] N. Karpukhina, et al., Chem. Soc. Rev. 43 (2014) 2174-2186.

[9] V. R. Mastelaro, et al., J. Mater. Sci. 54 (2019) 9313-9320.

[10] R. Choudhary, et al., Mater. Sci. Eng. C 68 (2016) 89-100.

[11] N.Y. Iwata, et al., MRS Online Proc. Libr. 599 (1999) 169-174

[12] N.Y. Iwata, et al., Colloids Surfaces B Biointerfaces 33 (2004) 1-6.

[13] S. Yamamoto, et al., Trans. Mater. Res. Soc. Japan 44 (2019) 17-23.

[14] A.E. Alecu, et al., Gels 8 (2022) 574.

[15] S.M. Naga, et al., Interceram. 68 (2019) 22-29.

[16] A.J. Salinas, et al., Key Eng. Mater. 391 (2009) 141-158.

[17] C. Migneco, et al., Materials 13 (2020) 540.

[18] A. Migdał-Mikuli, et al., J. Therm. Anal. Calorim. 89 (2007) 499-503.

[19] Q. Huang, et al., J. Anal. Appl. Pyrolysis 91 (2011) 159-164.

[20] R. Choudhary, et al., J. Asian Ceram. Soc. 8 (2020) 1-15.

[21] R. Choudhary, et al., J. Asian Ceram. Soc. 3 (2015) 173-177.

[22] A. Alecu, et al., Gels 8 (2022) 574.